

RESEARCH ARTICLE

# The complete plastid genomes of *Ophrys iricolor* and *O. sphegodes* (Orchidaceae) and comparative analyses with other orchids

Luca Roma<sup>1</sup>, Salvatore Cozzolino<sup>1\*</sup>, Philipp M. Schlüter<sup>2,3</sup>, Giovanni Scopece<sup>1</sup>, Donata Cafasso<sup>1</sup>

**1** Department of Biology, University Federico II of Naples, Complesso Universitario Monte Sant'Angelo, Naples, Italy, **2** Department of Systematic and Evolutionary Botany, University of Zurich, Zollikerstrasse 107, Zurich, Switzerland, **3** Institute of Botany, University of Hohenheim, Garbenstraße 30, Stuttgart, Germany

\* [cozzolin@unina.it](mailto:cozzolin@unina.it)



## Abstract

Sexually deceptive orchids of the genus *Ophrys* may rapidly evolve by adaptation to pollinators. However, understanding of the genetic basis of potential changes and patterns of relationships is hampered by a lack of genomic information. We report the complete plastid genome sequences of *Ophrys iricolor* and *O. sphegodes*, representing the two most species-rich lineages of the genus *Ophrys*. Both plastomes are circular DNA molecules (146754 bp for *O. sphegodes* and 150177 bp for *O. iricolor*) with the typical quadripartite structure of plastid genomes and within the average size of photosynthetic orchids. 213 Simple Sequence Repeats (SSRs) (31.5% polymorphic between *O. iricolor* and *O. sphegodes*) were identified, with homopolymers and dipolymers as the most common repeat types. SSRs were mainly located in intergenic regions but SSRs located in coding regions were also found, mainly in *ycf1* and *rpoC2* genes. The *Ophrys* plastome is predicted to encode 107 distinct genes, 17 of which are completely duplicated in the Inverted Repeat regions. 83 and 87 putative RNA editing sites were detected in 25 plastid genes of the two *Ophrys* species, all occurring in the first or second codon position. Comparing the rate of nonsynonymous (dN) and synonymous (dS) substitutions, 24 genes (including *rbcl* and *ycf1*) display signature consistent with positive selection. When compared with other members of the orchid family, the *Ophrys* plastome has a complete set of 11 functional *ndh* plastid genes, with the exception of *O. sphegodes* that has a truncated *ndhF* gene. Comparative analysis showed a large co-linearity with other related Orchidinae. However, in contrast to *O. iricolor* and other Orchidinae, *O. sphegodes* has a shift of the junction between the Inverted Repeat and Small Single Copy regions associated with the loss of the partial duplicated gene *ycf1* and the truncation of the *ndhF* gene. Data on relative genomic coverage and validation by PCR indicate the presence, with a different ratio, of the two plastome types (i.e. with and without *ndhF* deletion) in both *Ophrys* species, with a predominance of the deleted type in *O. sphegodes*. A search for this deleted plastid region in *O. sphegodes* nuclear genome shows that the deleted region is inserted in a retrotransposon nuclear sequence. The present study provides useful genomic tools for studying conservation and patterns of relationships of this rapidly radiating orchid genus.

## OPEN ACCESS

**Citation:** Roma L, Cozzolino S, Schlüter PM, Scopece G, Cafasso D (2018) The complete plastid genomes of *Ophrys iricolor* and *O. sphegodes* (Orchidaceae) and comparative analyses with other orchids. PLoS ONE 13(9): e0204174. <https://doi.org/10.1371/journal.pone.0204174>

**Editor:** Serena Aceto, University of Naples Federico II, ITALY

**Received:** June 4, 2018

**Accepted:** September 3, 2018

**Published:** September 18, 2018

**Copyright:** © 2018 Roma et al. This is an open access article distributed under the terms of the [Creative Commons Attribution License](https://creativecommons.org/licenses/by/4.0/), which permits unrestricted use, distribution, and reproduction in any medium, provided the original author and source are credited.

**Data Availability Statement:** The complete plastome sequences of *Ophrys sphegodes* and *O. iricolor* were deposited in the Sequence Reads Archive (NCBI-SRA) database under the accession number SRP148126.

**Funding:** This research was carried out in the frame of Programme STAR, financially supported by UniNA and Compagnia di San Paolo (GS) and Swiss National Science Foundation (SNF grant 31003A\_155943 to PMS).

**Competing interests:** The authors have declared that no competing interests exist.

## Introduction

Plastids such as chloroplasts are important plant organelles involved in the photosynthetic process thus providing essential energy to plants [1]. Plastids have small circular genomes, ranging from 135 to 160 kb [2–4]. Most angiosperm plastid genomes so far annotated have a quadripartite structure containing two copies of Inverted Repeat (IR) regions, separating a Large Single Copy (LSC) and Small Single Copy (SSC) regions [5–7]. Recently, with the extraordinary advances in sequencing platforms, many plastid genomes have been annotated and have provided valuable tools for the understanding of plant phylogenies and genome evolution e.g. [8]. Plastid structure and gene order are generally stable, and the rate of nucleotide substitution is slow [9] so that plastid genomes were traditionally considered to have experienced rearrangements rarely enough to be suitable to demarcate major plant groups [10]. Nonetheless, several angiosperm lineages show extensive gene order changes in plastid genomes that are often correlated with increased rates of nucleotide substitutions and gene and/or multiple intron losses [11, 12]. These rearrangements in the plastid genome have been found to be often associated with repeated sequences [2].

The family Orchidaceae consists of more than 700 genera and approximately 28,000 species [13], which are distributed in a wide variety of habitats. So far, several complete plastid genomes have been annotated in different orchid lineages. These studies revealed that Orchidaceae often underwent accelerated plastome evolution including large inversions, shifts in boundaries between IRs and the two single copies, indels, intron losses, and pseudogene formation by stop codons often associated with shifts from heterotrophy to parasitism/heterotrophism [14,15]. Compared to other angiosperms, photosynthetic orchids were also found particularly variable in the conservation of *NADH* dehydrogenase (*ndh*) genes [16], that encode components of the thylakoid complex involved in the redox level of the cyclic photosynthetic electron transporters.

The number of intact and degraded *ndh* genes present in the orchids plastomes varies even among closely related species suggesting that this specific gene class may be actively degraded in Orchidaceae [17]. This is not surprising as gene transfer from plastid to nucleus is known to occur frequently during evolutionary processes as even the complete loss of some plastid-encoded *ndh* genes seems to not affect the plant life [15]. Indeed, there is no clear-cut evidence of phylogenetic signal in the pseudogenization or loss of the *ndh* genes. For instance, no correlation with phylogeny was found for *ndh* genes loss in the Epidendroideae lineages while related species of Oncidiinae show a consistent loss of two *ndh* genes (*ndhF* and *ndhK*) and pseudogenization by gene truncation of other five genes (*ndhA*, D, H, I and J) [18].

The IR/SC junctions represent another hotspot of orchid plastome evolution, with the rearrangement of flanking regions leading to expansion or contraction of the inverted repeat regions. Different types of junctions have been reported in orchids, with considerable variation particularly in the *ycf1* gene [19]. It has been hypothesized that the exhibited usage bias of A/T base pairs typical of all known orchid *ycf1* genes would render less stable the DNA in the *ycf1* gene thus leading to the higher recombination of IR/SSC junction [20]. This often leads to a consequent partial or complete degradation of the *ndhF* gene, or even, in some case, to its transfer to mitochondrial DNA by intraorganellar recombination [17].

Despite Orchidaceae represents approximately 1/8 of all flowering plants [13], most published plastid sequences belong to tropical orchid lineages, while there is a remarkable dearth of information for the important temperate terrestrial subtribe Orchidinae with only two *Habenaria* and one *Platanthera* species plastomes having been annotated so far [17, 21]. With the aim to fill this gap, we sequenced the complete plastid genomes of *Ophrys iricolor* and *Ophrys sphegodes*. These species are representative of the two main diverging lineages of the

Mediterranean *Ophrys*, a sexually deceptive genus belonging to the subtribe Orchidinae characterized by an elevated taxonomic complexity due to a very fast radiation by pollinator shifts [22, 23]. The specific aims of the present study were to (i) annotate the complete plastid genome sequences of two *Ophrys* species, (ii) evaluate the homology between these two plastomes, (iii) investigate any significant characteristics suggesting plastome rearrangement in *Ophrys* and their phylogenetic signal, and (iv) explore significant changes in gene content and gene order in the subtribe Orchidinae compared to other orchid subtribes.

## Materials and methods

### Genome sequencing, assembling and annotation

DNA was extracted from a specimen of *Ophrys iricolor* (collected between Miamou and Agios Kyrillos, Crete, Greece; N34.9693, E24.9154; under permit number 118565/3022 issued by the Ministry of Environment and Energy in Athens on 13.02.2015) and from a specimen of *Ophrys sphegodes* (collected between Cagnano Varano and San Nicandro Garganico, Apulia, Italy; N41.9133, E15.6784 under permit number 173 issued by the National Park of Gargano in Monte Sant'Angelo (FG) on 12.01.2016). Whole genomic libraries were sequenced in paired-end mode, 2 x 150 bp, using the Illumina HiSeq 4000 platform (Illumina Inc., San Diego, CA, USA) at the Functional Genomics Centre Zurich (Switzerland). The obtained reads were trimmed using the software TRIMMOMATIC v. 0.36 [24] and the resulting trimmed reads (309,012,252 reads for *O. sphegodes* and 251,959,572 reads for *O. iricolor*) were *de novo* assembled using NOVOPLASTY v. 2.5.2 [25]. The gene annotation of the *Ophrys* plastid genomes was carried out using the software GESEQ v. 1.42 [26] and BLAST v. 2.6.0 [27] searches. From this initial annotation analysis, putative starts and stops of the gene exons, along with the positions of the related introns, were determined based on comparisons to homologous genes in other plastid genomes [28]. All tRNA genes were verified by using tRNAscan-SE server v. 1.3.1 [29]. The physical maps of the plastid circular genomes were drawn using Organellar Genome DRAW (OGDRAW) v. 1.2.1 [30]. The complete plastome sequences of *Ophrys sphegodes* and *O. iricolor* were deposited in the Sequence Reads Archive (NCBI-SRA) database under the accession number SRP148126. BLAST v. 2.6.0 [27, 31] was used to check whether deleted part of the *ndhF* gene in the *O. sphegodes* plastid genome was translocated into the nuclear genome. Reads were realigned against the assembled scaffolds of *O. sphegodes* nuclear genome (unpublished) using BWA v. 0.7.16 and converted in BAM [32] format using SAMtools v. 1.5 [33]. Finally, a BLASTX search was performed to annotate the nuclear *O. sphegodes* scaffold1075174.

### Genome structure, deletions validation, and repeat sequences

The software MAFFT v. 7.205 [34] and the Perl script Nucleotide MUMmer (NUCmer) available in MUMmer 3.0 [35] were employed to compare the plastome structures between *O. sphegodes* and *O. iricolor*. To detect putative errors in the *de novo* assemblies, the trimmed reads were mapped to the assembled genomes using the aligner BWA [32], converted to BAM format using SAMtools [33] and finally visualized using the IGV genome browser v. 2.4 [36]. To validate the deletion *in silico*, BAM files were further analysed using the software BEDtools coverage v. 2.21.0 [37] which generated a table in BED format containing an interval “windows” with coverage information across the two *Ophrys* plastomes. The BED file format was in turn used to visualize the sequencing coverage in regions of interest using the software CNView v. 1.0 [38]. To experimentally validate the *ndhF* deletion in *O. sphegodes/O. iricolor*, we designed primers for both the flanking and internal regions of *ndhF* from the assembled plastomes (S1A Fig). With these primers, we PCR amplified DNAs of *O. sphegodes* and *O.*

*iricolor* from different localities and of *O. incubacea* and *O. fusca*, as close relatives to *O. sphegodes* and *O. iricolor*, respectively and *O. insectifera* as distant related. PCR reaction conditions were as described in [39], with 5 ng of total DNA as template. Amplification products were visualized on 2% agarose gel using a 100 bp ladder as standard. PCR products and ladder were stained with ethidium bromide and photographed using a digital camera. Confirmatory sequences of the PCR products were done with ABI3130 automatic sequencer following manufacture instructions. Simple sequence repeats (SSRs) or microsatellites were detected using the MICroSATellite (MISA) Perl script v. 1.0 [40]. Thresholds were set at eight repeat units for mononucleotide SSRs, four repeat units for di- and trinucleotide SSRs, and three repeat units for tetra-, penta- and hexanucleotide SSRs as done in [41]. We also analysed tandem repeat sequences from the plastid genomes of *O. sphegodes* and *O. iricolor* and searched for forward, reverse and palindromic repeats by using REPuter [42]. We limited the maximum computed repeats and the minimal repeat size to 50 and 8, respectively and with a Hamming distance equal to 1.

### Prediction of RNA editing sites and identification of positive signatures in plastid protein-coding genes

Potential RNA editing sites in protein-coding genes of *Ophrys* plastome were predicted by the program PREPACT v. 2.0 [43] using the following 30 highly homologous reference genes from *Phalaenopsis aphrodite*: *accD*, *atpA*, *atpB*, *atpF*, *atpI*, *ccsA*, *clpP*, *matK*, *petB*, *petD*, *petG*, *petL*, *psaB*, *psaI*, *psbB*, *psbE*, *psbF*, *psbL*, *rpl2*, *rpl20*, *rpl23*, *rpoA*, *rpoB*, *rpoC1*, *rpoC2*, *rps2*, *rps8*, *rps14*, *rps16*, and *ycf3*.

In order to identify putative genes under positive selection, the 67 protein-coding genes present in sixteen Orchidaceae plastomes (*Ophrys iricolor*, AP018716 *O. sphegodes* AP018717, *Cattleya crispata* NC\_026568.1, *Corallorhiza odontorhiza* KM390021.1, *Cymbidium aloifolium* NC\_021429.1, *Cypripedium japonicum* KJ625630.1, *Goodyera procera* NC\_029363.1, *Habenaria pantlingiana* NC\_026775.1, *Masdevallia coccinea* NC\_026541.1, *Phalaenopsis aphrodite* NC\_017609.1, *Anoectochilus emeiensis* NC\_033895.1, *Apostasia wallichii* NC\_030722.1, *Dendrobium officinale* KX377961.1, *Phragmipedium longifolium* KM032625.1, *Platanthera japonica* MG925368.1, *Vanilla planifolia* KJ566306.1) were downloaded from Genbank. We analysed all coding gene regions, except *ndh* genes, due to their frequent loss across the entire set of orchids listed here.

In order to build a reference phylogenetic tree, all genes were aligned using MAFFT software v. 7.205 [44] and were concatenated using MESQUITE software v. 3.5 [45]. PARTITION FINDER software v. 2.1.0 [46] was used in order to search the best evolution model for each gene and a reference phylogenetic tree was built using RAxML software v. 8.2.10 using 1000 bootstrap replicates [47]. The positive signatures were analysed using SELECTON server v. 2.4 (<http://selecton.tau.ac.il/index.html>; [48], *Ophrys iricolor* was used as query sequence (i.e. the plastome type without *ndhF* deletion) and codon alignment was done using the software MAFFT v. 7.205 [44] implemented in SELECTON software. The phylogenetic tree was set as input in SELECTON analyses and branch lengths were automatically optimized from the software. The gene divergence was estimated by the sum of total branch lengths that link the operational taxonomical units to the common ancestor of Orchidaceae species sampled here as done in [28]. SELECTON software generated for each gene as output the number of putative sites under positive selection. In order to test whether positive selection is operating on a protein, a Likelihood Ratio Test for positive selection was performed with the comparison of M8 (allows positive selection) against M8a (null model). We consider in our analysis only sites where possible positive selection was inferred (lower bound > 1 and test with probability < 0.01). P-values

were adjusted for multiple testing in R (R Core Team) using FDR method in the *p.adjust* function.

## Results and discussion

### Genome organization and features

The plastomes of the two *Ophrys* species are circular DNA molecules of 146,754 bp for *O. sphegodes* and 150,177 bp for *O. iricolor* with the typical quadripartite structure of plastid genomes of flowering plants (Fig 1): a pair of inverted repeats of 25,052 bp and 26,348 bp, respectively, separated by a large single copy (LSC) region (80,471 bp and 80,541, respectively) and a small single copy (SSC) region of 16,179 bp and 16,940 bp, respectively for *O. sphegodes* (DDBJ accession number AP018717) and *O. iricolor* (DDBJ accession number AP018716). The size of the *Ophrys* plastid genome was comparable to other published plastomes of photosynthetic

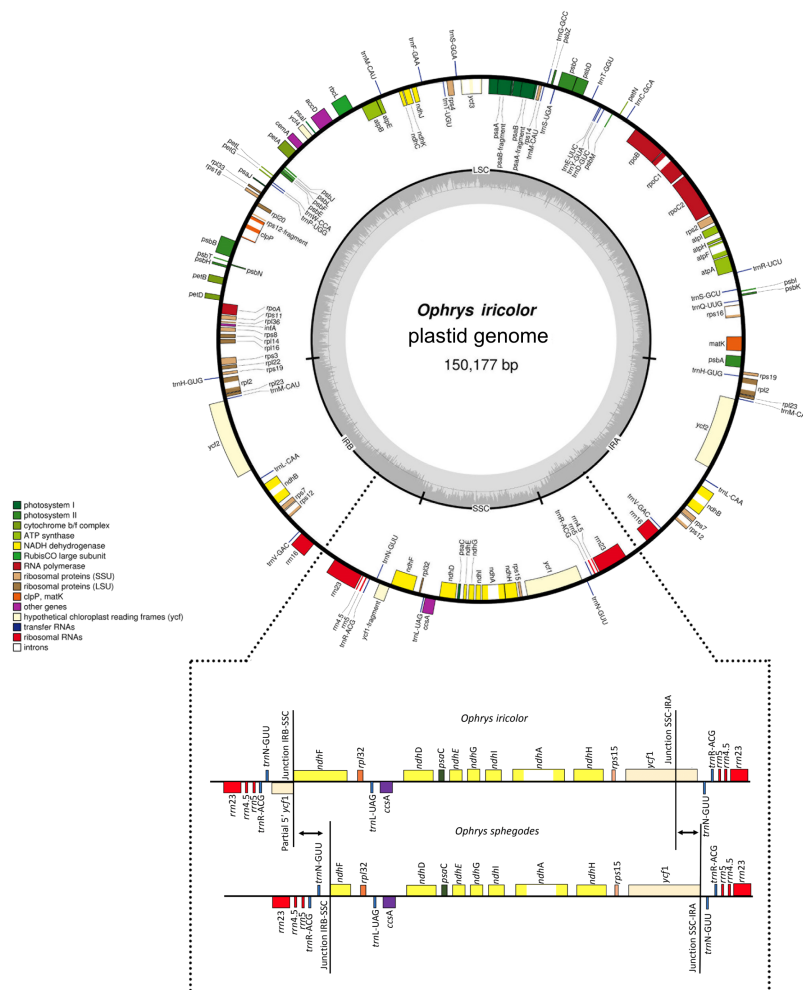


**Fig 1.** Gene map of *Ophrys sphegodes* (a) and *Ophrys iricolor* (b) plastid genomes. Genes drawn inside the circle are transcribed in the clockwise direction, and genes drawn outside are transcribed in the counter-clockwise direction. Different functional groups of genes are colour-coded. The darker grey in the inner circle corresponds to G/C content, and the lighter grey corresponds to A/T content. LSC, Large Single Copy; SSC, Small Single Copy; IRA/B, Inverted Repeat A/B. The enlargement shows that the loss of the partial duplicated gene of *ycf1* and the truncation of *ndhF* gene in *O. sphegodes* are correlated with the shift of the junction between the IR and SSC.

<https://doi.org/10.1371/journal.pone.0204174.g001>

orchids. The plastomes of the two *Ophrys* species are largely collinear with the exception of a large deletion in the *ndhF* gene in *O. sphegodes*.

The percentage of plastid reads in total WGS data was 5.43% for *O. sphegodes* and 1.96% for *O. iricolor*. The lowest average coverage of the assembled plastid genomes used was 13,673x for *O. sphegodes* and 3,816x for *O. iricolor*. The G/C contents were 37.14% and 36.4% respectively for *O. sphegodes* and *O. iricolor*, similar to other angiosperms (Table 1). The *Ophrys* plastome is predicted to encode 107 distinct genes, 17 of which are completely duplicated in the IR regions resulting in a total of 124 genes (Table 2). The annotation revealed distinct protein-coding genes (seven of them completely duplicated, namely *ndhB*, *rpl2*, *rpl23*, *rps7*, *rps12*, *rps19* and *ycf2*), 30 distinct tRNAs genes (five of them duplicated, *trnH-GUG*, *trnL-CAA*, *trnN-GUU*, *trnR-ACG*, *trnV-GAC* and one triplicated *trnM-CAU*), and four distinct rRNA genes (all of them completely duplicated: *rrn4.5*, *rrn5*, *rrn16* and *rrn23*). A truncated gene *ndhF*, was identified in *O. sphegodes* but not in *O. iricolor*. Ten genes contain one intron (*atpF*, *ndhA*, *ndhB*, *petB*, *petD*, *rpl2*, *rpl16*, *rps12*, *rps16* and *rpoC1*) and two genes (*clpP* and *ycf3*) contain two introns.

### Repeat sequence detection

The occurrence, type, and distribution of SSRs in *Ophrys* plastomes were analysed. In total, 213 SSRs were identified in *O. sphegodes* and *O. iricolor*. Three of these microsatellites occurred in the sequence portion that is deleted in *O. sphegodes* plastome (S1 Table). Homopolymers and dipolymers were the most common SSRs with, respectively, 71% and 24% occurrence. Seven and nine SSRs were present in compound formation in *O. iricolor* and *O. sphegodes*, respectively. Furthermore, the majority of *O. sphegodes* and *O. iricolor* SSRs are located in IGS regions (56.2% and 55%), followed by coding sequences (38.2% and 38%) and introns (5.6% and 7%), respectively. SSRs located in coding regions were found mainly in *ycf1* and *rpoC2* genes. A comparison of SSRs found in the two *Ophrys* species showed that 67 SSRs (31.5% of the total) were polymorphic between the two species. Among these polymorphic SSRs, 46 were located in the IGS regions, 5 in introns and 16 in genes (S1 Table).

*Ophrys sphegodes* contains 15 directed repeats, 9 inverted repeats, 3 complementary repeats and 21 palindromic repeats, whose lengths range from 18 to 60 bp. *Ophrys iricolor* contains 15 directed repeats, 27 palindromic repeats, 2 complementary repeats and 5 inverted repeats, whose lengths range from 20 to 60 bp. Most of the *O. iricolor* and *O. sphegodes* repeats were located in IGS regions (65.3% and 66.7% respectively), others were located in genes (22.4%, in *ycf2*, *petG*, *ndhC*, *psaA* and 22.9%; in *psbI*, *ndhC*, *ycf2*, *ndhA* respectively) and introns (12.3% and 10.4% in *clpP* and *rps16* intron respectively).

### RNA editing sites prediction and positive signatures of adaptive evolution

The RNA editing is a post-transcriptional modification typical of plastid and mitochondrial DNA. The process originated early during the evolution of land plants and several RNA

**Table 1. Comparison of two *Ophrys* plastid genomes.**

	<i>Ophrys sphegodes</i>	<i>Ophrys iricolor</i>
Plastid reads	16,782,955 bp	4,952,605 bp
Average plastid coverage	13,673 x	3,816 x
G/C percentage	37.14%	36.4%
Large Single Copy Region	80,471 bp	80,541 bp
Small Single Copy Region	16,179 bp	16,940 bp
Inverted Repeats	25,052 bp	26,348 bp

<https://doi.org/10.1371/journal.pone.0204174.t001>

**Table 2. List of genes identified in the plastomes of *Ophrys iricolor* and *Ophrys sphegodes*.**

Group of gene	Name of gene
Ribosomal RNA genes	<i>rrn16<sup>a</sup>; rrn23<sup>a</sup>; rrn4.5<sup>a</sup>; rrn5<sup>a</sup></i>
Transfer RNA Genes	<i>trnC-GCA; trnD-GUC; trnE-UUC; trnF-GAA; trnG-CCC; trnG-GCC; trnH-GUG<sup>a</sup>; trnL-CAA<sup>a</sup>; trnL-UAG; trnM-CAU<sup>c</sup>; trnN-GUU<sup>a</sup>; trnP-UGG; trnQ-UUG; trnR-ACG<sup>a</sup>; trnR-UCU; trnS-GCU; trnS-UGA; trnS-GGA; trnT-GGU; trnT-UGU; trnV-GAC<sup>a</sup>; trnW-CCA; trnY-GUA</i>
Small subunit of ribosome	<i>rps2; rps3; rps4; rps7<sup>a</sup>; rps8; rps11; rps12<sup>a</sup>; rps14; rps15; rps16; rps18; rps19<sup>a</sup></i>
Large subunit of ribosome	<i>rpl2<sup>a</sup>; rpl14; rpl16; rpl20; rpl22; rpl23<sup>a</sup>; rpl32; rpl33; rpl36</i>
DNA-dependent RNA polymerase	<i>rpoA; rpoB; rpoC1; rpoC2</i>
<i>Genes for photosynthesis:</i>	
Subunits of photosystem I (PSI)	<i>psaA; psaB; psaC; psaI; psaJ; ycf3; ycf4</i>
Subunits of photosystem II (PSII)	<i>psbA; psbB; psbC; psbD; psbE; psbF; psbH; psbI; psbJ; psbK; psbL; psbM; psbN; psbT; psbZ</i>
Subunits of cytochrome b <sub>6</sub> f	<i>petA; petB; petD; petG; petL; petN</i>
Subunits of ATP synthase	<i>atpA; atpB; atpE; atpF; atpH; atpI</i>
Subunits of NADH dehydrogenase	<i>ndhA; ndhB<sup>a</sup>; ndhC; ndhD; ndhE; ndhF<sup>b</sup>; ndhG; ndhH; ndhI; ndhK; ndhJ</i>
Large subunits of Rubisco	<i>rbcl</i>
<i>Other genes:</i>	
Maturase	<i>matK</i>
Envelope membrane protein	<i>cemA</i>
Subunit of acetyl-CoA carboxylase	<i>accD</i>
C-type cytochrome synthesis gene	<i>ccsA</i>
Protease	<i>clpP</i>
Component of TIC complex	<i>ycf1<sup>d</sup></i>
Translation initiation factor IF-1	<i>infA</i>
Genes of unknown function	<i>ycf2<sup>a</sup></i>

<sup>a</sup> Duplicated gene

<sup>b</sup> Truncated in *O. sphegodes*

<sup>c</sup> triplicated gene

<sup>d</sup> partially duplicated in *O. iricolor*

<https://doi.org/10.1371/journal.pone.0204174.t002>

editing sites have been maintained or lost during angiosperms evolution [49, 50]. In our analysis, PREPACT found a total of 83 and 87 putative RNA editing sites in 25 genes in *O. sphegodes* and *O. iricolor* respectively (S2 Table), in line with previous report for other orchids [51]. The RNA editing sites predicted for plastid genes of *Ophrys sphegodes* and *Ophrys iricolor* occur in the first or second codon position with all nucleotide changes being from cytidine (C) to uridine (U), as very often reported in other angiosperms. In *O. sphegodes* the genes predicted to have RNA editing sites are *matK* (12 sites), *rpoC1* (9 sites), *rpoC2* (8 sites), *rpoB* (8 sites), *accD* (6 sites), *rpoA* (4 sites), *atpA* (4 sites), *rpl2* (3 sites) *rpl20* (3 sites), *atpI* (3 sites), *ccsA* (3 sites), *ycf3* (3 sites), *clpP* (3 sites), *petB* (2 sites), *rps16* (2 sites) and the *atpF*, *petD*, *petL*, *psaB*, *psaI*, *psbF*, *rpl23*, *rps2*, *rps8* and *rps14* genes with only one site. In *O. iricolor* the genes predicted were the same as *O. sphegodes* with few differences: *ccsA* (5 sites), *atpA* (3 sites), *psaB* (2 sites), *rps14* (2 sites), *atpF* (2 sites) (S2 Table) which suggest a general conservation of the RNA editing mechanism within *Ophrys* but also that RNA editing evolution accumulated enough

differences to differentiate two *Ophrys* species. A previous study has also found that the number of RNA editing sites predicted for protein-coding genes in orchids species is high in comparison with other monocots [51]. Likelihood ratio test between a null model and an alternative model carried out following [52] shows that 24 genes are under positive selection (S3 Table); overall, the most divergent genes have the stronger signatures of positive selection (S2 Fig). In details, the positively selected genes were involved in different essential functions such as photosynthesis, PSII (*psbA*, *psbB*, *psbE*, *psbH*, *psbM*, *psbN* genes), large subunits of rubisco (*rbcL*), ATP synthase (*atpI* gene), cytochrome b6f (*petB* gene), subunits of RNA polymerase (*rpoA*, *rpoB*, *rpoC1*, *rpoC2* genes), RNA maturation (*matK* gene), ribosomal proteins (*rpl20*, *rpl22*, *rpl32*, *rpl33*, *rps12*, *rps19* genes), fatty acid biosynthesis (*accD* gene), cytochrome biosynthesis (*ccsA* gene), import of protein in the plastid (*ycf1* gene), and unknown function (*ycf2* gene). The high number of genes containing positive signatures (including the *rbcL* gene) among photosynthesis-related genes are consistent with previous observation on other monocots and may be related to the recent increase of diversification rate following adaptation to different ecological conditions. [53]. In particular, and as already suggested for other monocots as *Arecaceae*, many tropical orchid species grow as epiphytes in tropical forests and are shade adapted. The transition to the terrestrial habitus of all temperate orchid lineages (as *Ophrys*) may have promoted a new selective pressure for improving the photosynthesis efficiency under the new terrestrial ecological conditions [52].

Interestingly, some positively selected sites that were identified in our study (e.g., the *accD* and *ycf1* genes) have been found very variable also in other orchids and flowering plants [54]. In particular *accD* gene is a conserved plastid gene involved in de novo synthesis of fatty acids [55] and is essential for chloroplast functionality, leaf development and longevity [56]. Therefore *accD* has been associated in a significant manner with adaptation to the environment, including factors such as temperature, light, humidity, and atmosphere [57].

On the other hand, *ycf1* is one of the largest plastid genes and it has been found extremely divergent in orchids plastomes [19], likely because of its position at IR/SC junction that generates large variation in sequence length and pseudogenes [58] as also found in our study.

## Genomic comparison of *Ophrys* with other orchid plastomes

The *Ophrys* plastid genome is fully collinear both in gene order and gene orientation with the other available Orchidoideae. When compared with representative species belonging to the different subfamilies of the Orchidaceae (i.e., Epidendroideae, Cyripedioideae, Vanilloideae and Apostasioideae), we found that Cyripedioideae, Epidendroideae, Vanilloideae and Orchidoideae are largely collinear in plastid sequence with a few small exceptions: an inversion of the *psbM*—*petN* gene order in Epidendroideae and a gene inversion in the SSC of *Vanilla* (S3 Fig).

In contrast to these four tribes, large rearrangements in gene order have been found in the supposed basal smaller tribe of Apostasioideae. However, under the assumption that the common plastid types observed in most orchids represent the primitive state, it is likely that the rearrangements found in *Apostasia wallichii* and *Apostasia odorata* (but not in the related *Neuwiedia* [59]) may be due to recent, terminal autoapomorphic changes rather than being representative of the ancestral gene order of the orchid family.

As many *ndh* genes had either truncations or indels, resulting in frameshifts or pseudogenes in several orchid plastomes, we also compared *ndh* genes in the different tribes. *Ophrys iricolor*, like other Orchidoideae, has the complete set of *ndh* plastid genes, i.e. 11 functional genes, which is different from *Apostasia wallichii* and *Vanilla planifolia* in which the *ndhB* gene is

truncated and from *Vanilla planifolia* where all other 10 *ndh* subunits are deleted. The presence of *ndh* genes within terrestrial Orchidoideae is ubiquitous, which contrasts with the extensive variation in presence/absence of *ndh* genes found within tropical orchid genera (see *Cymbidium* [17]). The functional role of the *ndh* genes seems closely related to the land adaptation of photosynthesis so they have been conserved in terrestrial, temperate orchid plastomes whereas they are partially lost in epiphytic, tropical orchid plastomes [60].

### Boundaries between single copy and inverted repeat regions

Expansion or contraction of the IR region is one of the main causes of size variation among angiosperm plastid genomes [61] and it has found to be variable even among related orchid species as, for instance, within the *Cymbidium* genus [17]. The multiple genome alignment analysis using plastome sequences of *O. sphegodes* and *O. iricolor* revealed the loss of a *ycf1* fragment in the IR and partial deletion of the *ndhF* gene in *O. sphegodes* (S4 Fig). *In silico* validation confirmed the partial *ndhF* gene loss in *O. sphegodes* and demonstrated that part of the *ycf1* gene is duplicated in *O. iricolor*, which does not occur in *O. sphegodes* (Fig 2).

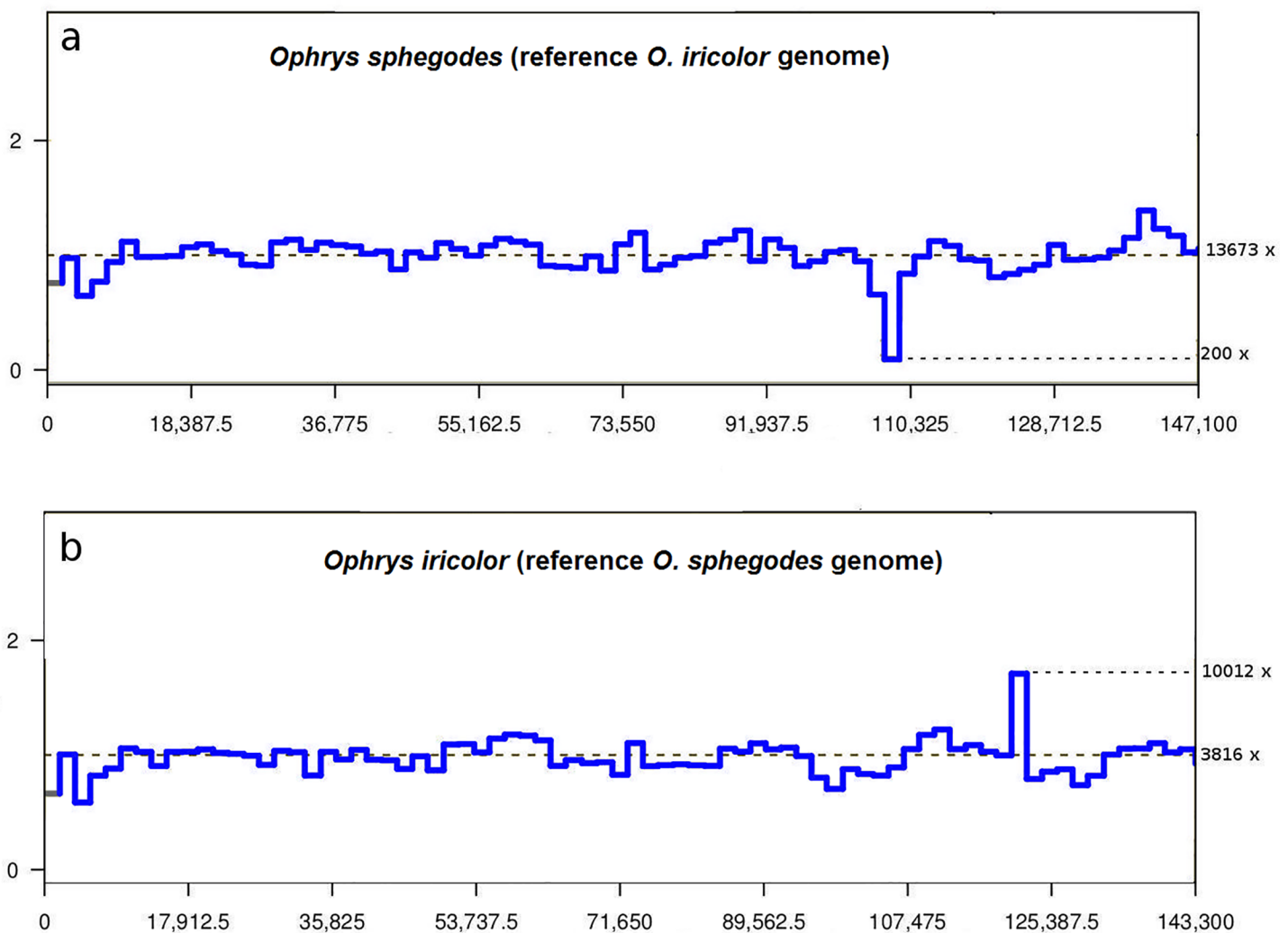


**Fig 2.** *In silico* validation of *ndhF* deletion (using software CNView) comparing *O. sphegodes* plastid reads against reference genome of *O. iricolor* (a) and *O. iricolor* plastid reads against reference genome of *O. sphegodes* (b). Y-axis represents normalized coverage values.

<https://doi.org/10.1371/journal.pone.0204174.g002>

In *O. sphegodes*, the loss of the partial duplicated gene of *ycf1* and the partial deletion of *ndhF* gene are correlated with the shift of the junction between the IR and SSC (Fig 1) with a pattern very similar to some *Cymbidium* species [17]. High sequence variability, especially in the *ycf1* gene at IR-SSC junction, have been frequently observed as a result of expansion and contractions events by gene conversion [62, 63]. While *in silico* validation by CNVIEW largely confirms the occurrence of the *ndhF* deletion in *O. sphegodes*, however, approximately 2% of *O. sphegodes* reads map on the plastid region corresponding to *O. iricolor* plastome type (i.e. where complete *ndhF* occurs). At the same time, IGV also reveals that 888 of *O. iricolor* reads map on the junction with *ndhF* deletion (i.e. corresponding to *O. sphegodes* plastome type). Thus, to confirm the occurrence of *ndhF* deletion in *O. sphegodes/O. iricolor*, we amplified DNA with primers for both the flanking and internal regions of *ndhF*. Further, to rule out any possible cross contamination (during the NGS steps) as cause of presence of both plastome types in both *Ophrys* species, different accessions were used in PCR validation. PCR amplifications with primers flanking *ndhF* yielded two amplicons in *O. iricolor*: a small one (0.25 Kb), corresponding to the plastid fragment with the *ndhF* deletion, and a larger amplicon (3.25 Kb) containing the undeleted *ndhF* gene. Only the small plastid fragment with the *ndhF* deletion (primers F1/R1) was detected in *O. sphegodes*. To exclude, in *O. sphegodes*, that the small fragment was selectively amplified due to its shorter size and higher copy number, we also amplified *O. sphegodes* and *O. iricolor* (as control) with primers located within the *ndhF* deletion (primers F2/R2). Contrary to expectation (i.e. no amplification in *O. sphegodes*) both species successfully amplified a 1.2 Kb fragment. However, the two species differed in their amplicon yield, i.e. we obtained a stronger amplification band in *O. iricolor* compared to *O. sphegodes* (S1 Fig b). Taken together, this suggest that both species contained copies with and without the *ndhF* deletion but with a different relative representation (high proportion of deletions in *O. sphegodes* and low in *O. iricolor*). The fact that all examined members of *O. sphegodes* and *O. iricolor* lineages (including the basal *O. insectifera*) share a similar PCR amplification pattern suggests that the deletion of *ndhF* has likely occurred only once during the early evolution of the genus *Ophrys*, i.e. immediately before the separation of the two main lineages. The presence of two plastome types (with a different relative representation) across the two lineages represents an unusual case of maintenance of plastid heteroplasmy likely established as consequence of retention of ancestral polymorphism or of plastid capture by hybridization. Both processes have been commonly suggested to explain the unusual genomic admixture detected among *Ophrys* species as they are characterized by very rapid radiation and recurrent hybridization [64, 65].

### Genomic localization of deleted *ndhF* gene in *O. sphegodes* nuclear genome

BLAST search of the assembly for the deleted *ndhF* region from the plastid genome of *O. sphegodes* found the nuclear scaffold1075174 (length 5,436 bp) with a score of 924 and e-value of 0.0. Reads of whole genome sequencing were mapped against scaffold1075174 to check whether some reads overlap with the junction between plastid deleted region and the remaining part of this scaffold. A total of 124,961 reads mapped on the scaffold. BLASTX search for the scaffold1075174 (after excluding the deleted plastid region) revealed the presence of a reverse transcriptase, a GAG pre-integrase domain, and the gag-polyprotein of LTR copia-type. Twelve reads map on the junction between *ndhF* and the reverse transcriptase so confirming the connection between the two parts. This result represents a clear indication that the deleted plastid region has been inserted in a retrotransposon nuclear sequence of *O. sphegodes* (Fig 3). Most of the repetitive DNA in available orchid genomes are gypsy- and copia-like retrotransposons [66] and their activity is likely to significantly contributed to the orchid large genome size [67].



Fig 3. Results of BLASTX search of scaffold1075174 (length 5,436 bp): Putative domain hits are indicated by the colored arrows.

<https://doi.org/10.1371/journal.pone.0204174.g003>

## Conclusions

The complete plastid genomes provided here for two taxa from the rapidly evolving orchid genus *Ophrys* represents a source of novel information that can help resolve evolutionary questions. While the plastid gene order and organization reveal the signal of phylogenetic relationships among main species groups in this genus, the highly variable SSRs and tandem repeats with suitable level of intraspecific variation can be used as markers in phylogeographic and speciation studies among those closely related species. These relationships can now be explored with the novel genomic resources available today.

## Supporting information

**S1 Table. Distribution of simple sequence repeat (SSR) in *Ophrys sphegodes* and *O. iricolor* plastid genomes.** IGS: intergenic spacer.

(DOCX)

**S2 Table. List of RNA editing sites predicted in protein-coding genes of *Ophrys* plastomes using PREPACT program.** High dashes indicate absence of RNA editing, \* stop codon.

(DOCX)

**S3 Table. Positive selection sites identified with selecton with d.f. = 1.** “Null” and “positive” columns list likelihood values obtained under the models M8a (null model) and M8 (positive selection), respectively.

(DOCX)

**S1 Fig. PCR validation of the *ndhF* deletion.** PCR amplifications using (a) F1 and R1 primers; (b) F2 and R2 primers. M = marker II ( $\lambda$  DNA / *Hind* III digested); 1 = *O. fusca* Campania, 2 = *O. fusca* Tuscany, 3 = *O. iricolor* Greece; 4 = *O. sphegodes* Campania; 5 = *O. sphegodes* Apulia; 6 = *O. incubacea* Apulia; 7 = *O. insectifera* Spain. A dotted line represents the IRB-SSC junction. Primer sequences:

F1: 5' -GCTCCGTTCCATGCCTCATT- 3'

R1: 5' -TCGTTCGTATGT GGGCTTTCC- 3'

F2: 5' -TTAGCAATTGCACCGACAAA- 3'

R2: 5' -TCTGTTTCCACCG GACAG- 3'.

(TIFF)

**S2 Fig.** Molecular evolution analyses of *Ophrys* plastid genes: a) divergence of protein-coding genes (gene divergence was estimated by the sum of total branch lengths in each gene tree inferred, mean  $\pm$  SD); b) number of putative sites under positive selection.

(TIF)

**S3 Fig. Comparison of gene rearrangements in the plastid genomes among 10 species representative of the five Orchid subfamilies.** Genes are indicated in the colored boxes. Boxes colors represent gene families: purple = photosystem I; yellow = photosystem II; orange = NADH-dehydrogenase; light green = ribosome large subunit; light blue = ribosome small

subunit; light red = rubisco subunit; red = RNA polymerase; green = ATP synthase; pink = cytochrome b/f complex; dark grey = acetyl-CoA carboxylase; light grey = hypothetical plastid reading frame (ycf series), protease, translation initiation factor IF-1; dark purple = maturase; dark blue = envelope membrane protein.  
(TIFF)

**S4 Fig. Dot-plot analyses of *Ophrys sphegodes* and *O. iricolor* plastid genomes using Mummer software.** A positive slope indicates that compared sequences are in the same orientation; a negative slope indicates that compared sequences can be aligned, but their orientation is opposite. Red: Sequences in the same direction; Blue: inversions.  
(JPG)

## Acknowledgments

This research was carried out in the frame of Programme STAR, financially supported by UniNA and Compagnia di San Paolo, as well as the Swiss National Science Foundation (SNF grant 31003A\_155943 to PMS). We thank Catharine Aquino (Functional Genomics Centre Zurich) for help with Illumina library preparation and Riccardo Aiese Cigliano and Walter Sanseverino (Sequentia Biotech sl) for bioinformatics support.

## Author Contributions

**Conceptualization:** Salvatore Cozzolino, Philipp M. Schlüter.

**Data curation:** Donata Cafasso.

**Funding acquisition:** Salvatore Cozzolino, Philipp M. Schlüter, Giovanni Scopece.

**Investigation:** Luca Roma.

**Methodology:** Luca Roma, Philipp M. Schlüter, Giovanni Scopece, Donata Cafasso.

**Supervision:** Donata Cafasso.

**Writing – original draft:** Luca Roma, Salvatore Cozzolino, Giovanni Scopece.

**Writing – review & editing:** Philipp M. Schlüter, Donata Cafasso.

## References

1. Raven JA, Allen JF (2003) Genomics and chloroplast evolution: what did cyanobacteria do for plants? *Genome Biology* 4: 209. PMID: [12620099](https://pubmed.ncbi.nlm.nih.gov/12620099/)
2. Palmer JD (1991) Plastid chromosomes: structure and evolution. In: Vasil LK, Bogorad L, editors. *Cell Culture and Somatic Cell Genetics in Plants, the Molecular Biology of Plastid 7A*. San Diego: Academic Press; pp. 5–53.
3. Downie SR, Palmer JD (1992) Use of chloroplast DNA rearrangements in reconstructing plant phylogeny. In: Soltis PS, Soltis DE, Doyle JJ, editors. *Molecular Systematics of Plants*. Springer US; pp. 14–35.
4. Judd WS, Campbell CS, Kellogg EA, Stevens PF, Donoghue MJ (2002) *Plant systematics: a phylogenetic approach*. 2nd ed. Sunderland, Massachusetts: Sinauer Associates.
5. Chaney L, Mangelson R, Ramaraj T, Jellen EN, Maughan PJ (2016) The complete chloroplast genome sequences for four *Amaranthus* species (Amaranthaceae). *Applications in Plant Sciences* 4.
6. Cho KS, Cheon KS, Hong SY, Cho JH, Im JS, Mekapogu M, et al. (2016) Complete chloroplast genome sequences of *Solanum commersonii* and its application to chloroplast genotype in somatic hybrids with *Solanum tuberosum*. *Plant Cell Reports* 35: 2113–2123. <https://doi.org/10.1007/s00299-016-2022-y> PMID: [27417695](https://pubmed.ncbi.nlm.nih.gov/27417695/)

7. Fu J, Liu H, Hu J, Liang Y, Liang J, Wuyun T, Tan X (2016) Five complete chloroplast genome sequences from diospyros: genome organization and comparative analysis. *PLoS One* 11: e0159566. <https://doi.org/10.1371/journal.pone.0159566> PMID: 27442423
8. Xu J-H, Liu Q, Hu W, Wang T, Xue Q, Messing J (2015) Dynamics of chloroplast genomes in green plants. *Genomics* 106: 221–231. <https://doi.org/10.1016/j.ygeno.2015.07.004> PMID: 26206079
9. Wolfe K, Li W, Sharp P (1987) Rates of Nucleotide Substitution Vary Greatly among Plant Mitochondrial, Chloroplast, and Nuclear DNAs. *Proceedings of the National Academy of Sciences USA* 84: 9054–9058.
10. Shaw J, Lickey EB, Schilling EE, Small RL (2007) Comparison of whole chloroplast genome sequences to choose noncoding regions for phylogenetic studies in angiosperms: the tortoise and the hare III. *American Journal of Botany* 94: 275–288. <https://doi.org/10.3732/ajb.94.3.275> PMID: 21636401
11. Kang JS, Lee BY, Kwak M (2017) The complete chloroplast genome sequences of *Lychnis wilfordii* and *Silene capitata* and comparative analyses with other Caryophyllaceae genomes. *PLoS one* 12: e0172924. <https://doi.org/10.1371/journal.pone.0172924> PMID: 28241056
12. Jansen RK, Cai Z, Raubeson LA, Daniell H, Leebens-Mack J, Müller KF et al. (2007) Analysis of 81 genes from 64 plastid genomes resolves relationships in angiosperms and identifies genome-scale evolutionary patterns. *Proceedings of the National Academy of Sciences USA* 104: 19369–19374.
13. Christenhusz MJM, Byng JW (2016) The number of known plants species in the world and its annual increase. *Phytotaxa* 261: 201–217.
14. Barrett CF, Freudenstein JV, Li J, Mayfield-Jones DR, Perez L, Pires JC, Santos C (2014) Investigating the path of plastid genome degradation in an early-transitional clade of heterotrophic orchids, and implications for heterotrophic angiosperms. *Molecular Biology and Evolution* 31: 3095–3112. <https://doi.org/10.1093/molbev/msu252> PMID: 25172958
15. Lin CS, Chen JJ, Huang YT, Chan MT, Daniell H, Chang WJ et al. (2015) The location and translocation of *ndh* genes of chloroplast origin in the Orchidaceae family. *Scientific Reports* 5: 9040. <https://doi.org/10.1038/srep09040> PMID: 25761566
16. Luo J, Hou BW, Niu ZT, Liu W, Xue QY, Ding XY (2014) Comparative chloroplast genomes of photosynthetic orchids: insights into evolution of the Orchidaceae and development of molecular markers for phylogenetic applications. *PLoS One* 9: e99016. <https://doi.org/10.1371/journal.pone.0099016> PMID: 24911363
17. Kim HT, Chase MW (2017) Independent degradation in genes of the plastid *ndh* gene family in species of the orchid genus *Cymbidium* (Orchidaceae; Epidendroideae). *PLoS One* 12: e0187318. <https://doi.org/10.1371/journal.pone.0187318> PMID: 29140976
18. Wu FH, Chan MT, Liao DC, Hsu CT, Lee YW, Daniell H et al. (2010) Complete chloroplast genome of *Oncidium* Gower Ramsey and evaluation of molecular markers for identification and breeding in *Oncidinae*. *BMC Plant Biology* 10: 68. <https://doi.org/10.1186/1471-2229-10-68> PMID: 20398375
19. Neubig KM, Whitten WM, Carlsward BS, Blanco MA, Endara L, Williams NH, Moore M (2009) Phylogenetic utility of *ycf1* in orchids: a plastid gene more variable than *matK*. *Plant Systematics and Evolution* 277: 75–84.
20. Wang RJ, Cheng CL, Chang CC, Wu CL, Su TM, Chaw SM (2008) Dynamics and evolution of the inverted repeat-large single copy junctions in the chloroplast genomes of monocots. *BMC Evolutionary Biology* 8: 36. <https://doi.org/10.1186/1471-2148-8-36> PMID: 18237435
21. Dong WL, Wang RN, Zhang NY, Fan WB, Fang MF, Li ZH (2018) Molecular Evolution of Chloroplast Genomes of Orchid Species: Insights into Phylogenetic Relationship and Adaptive Evolution. *International Journal of Molecular Sciences* 19: 716.
22. Devey DS, Bateman RM, Fay MF, Hawkins JA (2008) Friends or relatives? Phylogenetics and species delimitation in the controversial European orchid genus *Ophrys*. *Annals of Botany* 101: 385–402. <https://doi.org/10.1093/aob/mcm299> PMID: 18184645
23. Breitkopf H, Onstein RE, Cafasso D, Schlüter PM, Cozzolino S (2015) Multiple shifts to different pollinators fuelled rapid diversification in sexually deceptive *Ophrys* orchids. *New Phytologist* 207: 377–389. <https://doi.org/10.1111/nph.13219> PMID: 25521237
24. Bolger AM, Lohse M, Usadel B (2014) Trimmomatic: a flexible trimmer for Illumina Sequence Data. *Bioinformatics* 30: 2114–2120. <https://doi.org/10.1093/bioinformatics/btu170> PMID: 24695404
25. Dierckxsens N, Mardulyn P, Smits G (2017) NOVOPlasty: *de novo* assembly of organelle genomes from whole genome data. *Nucleic Acids Research* 45: e18. <https://doi.org/10.1093/nar/gkw955> PMID: 28204566
26. Tillich M, Lehwark P, Pellizzer T, Ulbricht-Jones ES, Fischer A, Bock R, Greiner S (2017) GeSeq—versatile and accurate annotation of organelle genomes. *Nucleic Acids Research* 45: W6–W11. <https://doi.org/10.1093/nar/gkx391> PMID: 28486635

27. Altschul SF, Gish W, Miller W, Myers EW, Lipman DJ (1990) Basic local alignment search tool. *Journal of Molecular Biology* 215: 403–410. [https://doi.org/10.1016/S0022-2836\(05\)80360-2](https://doi.org/10.1016/S0022-2836(05)80360-2) PMID: 2231712
28. de Santana Lopes A, Pacheco TG, do Nascimento Vieira L, Guerra MP, Nodari RO, de Souza EM et al. (2018) The *Crambe abyssinica* plastome: Brassicaceae phylogenomic analysis, evolution of RNA editing sites, hotspot and microsatellite characterization of the tribe Brassiceae. *Gene* 671: 36–49.
29. Lowe TM, Eddy SR (1997) tRNAscan-SE: A program for improved detection of transfer RNA genes in genomic sequence. *Nucleic Acids Research* 25: 955–964. PMID: 9023104
30. Lohse M, Drechsel O, Kahlau S, Bock R (2013) OrganellarGenomeDRAW—a suite of tools for generating physical maps of plastid and mitochondrial genomes and visualizing expression data sets. *Nucleic Acids Research* 41: W575–W581. <https://doi.org/10.1093/nar/gkt289> PMID: 23609545
31. Luo R, Liu B, Xie Y, Li Z, Huang W, Yuan J et al. (2012) SOAPdenovo2: an empirically improved memory-efficient short-read de novo assembler. *Gigascience* 1: 18. <https://doi.org/10.1186/2047-217X-1-18> PMID: 23587118
32. Li H, Durbin R (2009) The short read alignment component (bwa-short) has been published: Fast and accurate short read alignment with Burrows-Wheeler Transform. *Bioinformatics* 25: 1754–1760. <https://doi.org/10.1093/bioinformatics/btp324> PMID: 19451168
33. Li H, Handsaker B, Wysoker A, Fennell T, Ruan J, Homer N, Marth G, Abecasis G, Durbin R and 1000 Genome Project Data Processing Subgroup (2009) The Sequence alignment/map (SAM) format and SAMtools. *Bioinformatics* 25: 2078–2079. <https://doi.org/10.1093/bioinformatics/btp352> PMID: 19505943
34. Katoh K, Rozewicki J, Yamada KD (2017) MAFFT online service: multiple sequence alignment, interactive sequence choice and visualization. *Briefings in Bioinformatics* bbx108.
35. Kurtz S, Phillippy A, Delcher AL, Smoot M, Shumway M, Antonescu C, Salzberg SL (2004) Versatile and open software for comparing large genomes. *Genome Biology* 5: R12. <https://doi.org/10.1186/gb-2004-5-2-r12> PMID: 14759262
36. Thorvaldsdóttir H, Robinson JT, Mesirov JP (2013) Integrative Genomics Viewer (IGV): high-performance genomics data visualization and exploration. *Briefings in Bioinformatics* 14: 178–192. <https://doi.org/10.1093/bib/bbs017> PMID: 22517427
37. Quinlan AR, Hall IM (2010) BEDTools: a flexible suite of utilities for comparing genomic features. *Bioinformatics* 26: 841–842. <https://doi.org/10.1093/bioinformatics/btq033> PMID: 20110278
38. Collins RL, Stone MR, Brand H, Glessner JT, Talkowski ME (2016) CNView: a visualization and annotation tool for copy number variation from whole-genome sequencing. *bioRxiv* 049536.
39. Cozzolino S, Cafasso D, Pellegrino G, Musacchio A, Widmer A (2003) Molecular evolution of a plastid tandem repeat locus in an orchid lineage. *Journal of Molecular Evolution* 57: S41–S49. <https://doi.org/10.1007/s00239-003-0006-3> PMID: 15008402
40. Thiel T, Michalek W, Varshney R, Graner A (2003) Exploiting EST databases for the development and characterization of gene-derived SSR-markers in barley (*Hordeum vulgare* L.). *Theoretical and Applied Genetics* 106: 411–422. <https://doi.org/10.1007/s00122-002-1031-0> PMID: 12589540
41. de Santana Lopes A, Pacheco TG, dos Santos KG, do Nascimento Vieira L, Guerra MP, Nodari RO et al. (2018). The *Linum usitatissimum* L. plastome reveals atypical structural evolution, new editing sites, and the phylogenetic position of Linaceae within Malpighiales. *Plant cell reports*, 37: 307–328. <https://doi.org/10.1007/s00299-017-2231-z> PMID: 29086003
42. Kurtz S, Schleiermacher C (1999) REPuter: fast computation of maximal repeats in complete genomes. *Bioinformatics* 15: 426–427. PMID: 10366664
43. Lenz H, Rüdinger M, Volkmar U, Fischer S, Herres S, Grewe F, Knoop V (2010) Introducing the plant RNA editing prediction and analysis computer tool PREPACT and an update on RNA editing site nomenclature. *Current Genetics* 56: 189–201. <https://doi.org/10.1007/s00294-009-0283-5> PMID: 20041252
44. Katoh K, Misawa K, Kuma K, Miyata T (2002) MAFFT: a novel method for rapid multiple sequence alignment based on fast Fourier transform. *Nucleic Acids Research* 30: 3059–3066. PMID: 12136088
45. Maddison WP, Maddison DR (2018) Mesquite: a modular system for evolutionary analysis. Version 3.40 <http://mesquiteproject.org>.
46. Lanfear R, Frandsen PB, Wright AM, Senfeld T, Calcott B (2016) PartitionFinder 2: new methods for selecting partitioned models of evolution for molecular and morphological phylogenetic analyses. *Molecular Biology and Evolution* 34: 772–773.
47. Stamatakis A (2014) RAxML version 8: a tool for phylogenetic analysis and post-analysis of large phylogenies. *Bioinformatics* 30: 1312–1313. <https://doi.org/10.1093/bioinformatics/btu033> PMID: 24451623

48. Stern A, Doron-Faigenboim A, Erez E, Martz E, Bacharach E, Pupko T (2007) Selecton 2007: advanced models for detecting positive and purifying selection using a Bayesian inference approach. *Nucleic Acids Research* 35: W506–W511. <https://doi.org/10.1093/nar/gkm382> PMID: 17586822
49. Tillich M, Lehwark P, Morton BR, Maier UG (2006) The evolution of chloroplast RNA editing. *Molecular Biology and Evolution* 23: 1912–1921. <https://doi.org/10.1093/molbev/msl054> PMID: 16835291
50. Takenaka M, Zehrmann A, Verbitskiy D, Härtel B, Brennicke A (2013) RNA editing in plants and its evolution. *Annual Review of Genetics* 47: 335–352. <https://doi.org/10.1146/annurev-genet-111212-133519> PMID: 24274753
51. Chen TC, Liu YC, Wang X, Wu CH, Huang CH, Chang CC (2017) Whole plastid transcriptomes reveal abundant RNA editing sites and differential editing status in *Phalaenopsis aphrodite* subsp. *formosana*. *Botanical Studies* 58: 38. <https://doi.org/10.1186/s40529-017-0193-7> PMID: 28916985
52. de Santana Lopes A, Gomes Pacheco G, Nimz T, do Nascimento Vieira L, Guerra MP, Nodari RO et al. (2018). The complete plastome of macaw palm [*Acrocomia aculeata* (Jacq.) Lodd. ex Mart.] and extensive molecular analyses of the evolution of plastid genes in Arecaceae. *Planta* 247: 1011–1030. <https://doi.org/10.1007/s00425-018-2841-x> PMID: 29340796
53. Piot A, Hackel J, Christin PA, Besnard G (2017) One-third of the plastid genes evolved under positive selection in PACMAD grasses. *Planta* 247: 255–266. <https://doi.org/10.1007/s00425-017-2781-x> PMID: 28956160
54. Givnish TJ, Spalink D, Ames M, Lyon SP, Hunter SJ, Zuluaga A et al. (2015) Orchid phylogenomics and multiple drivers of their extraordinary diversification. *Proceedings of the Royal Society of London B* 282: 2108–2111.
55. Feria Bourrellier AB, Valot B, Guillot A, Ambard-Bretteville F, Vidal J, Hodges M (2010) Chloroplast acetyl-CoA carboxylase activity is 2-oxoglutarateregulated by interaction of PII with the biotin carboxyl carrier subunit. *Proceedings of the National Academy of Science U S A* 107: 502–507.
56. Mizoi J, Nishida I, Nagano Y, Sasaki Y (2002) Chloroplast transformation with modified accD operon increases acetyl-CoA carboxylase and causes extension of leaf longevity and increase in seed yield in tobacco. *Plant Cell Physiology* 43: 1518–1525. PMID: 12514249
57. Hu S, Sablok G, Wang B, Qu D, Barbaro E, Viola R et al. (2015) Plastome organization and evolution of chloroplast genes in *Cardamine* species adapted to contrasting habitats. *BMC Genomics* 16: 306. <https://doi.org/10.1186/s12864-015-1498-0> PMID: 25887666
58. Jheng CF, Chen TC, Lin JY, Chen TC, Wu WL, Chang CC (2012) The comparative chloroplast genomic analysis of photosynthetic orchids and developing DNA markers to distinguish *Phalaenopsis* orchids. *Plant Science* 190: 62–73. <https://doi.org/10.1016/j.plantsci.2012.04.001> PMID: 22608520
59. Niu Z, Pan J, Zhu S, Li L, Xue Q, Liu W, Ding X (2017) Comparative analysis of the complete plastomes of *Apostasia wallichii* and *Neuwiedia singaporeana* (Apostasioideae) reveals different evolutionary dynamics of IR/SSC boundary among photosynthetic orchids. *Frontiers in Plant Science* 8: 1713. <https://doi.org/10.3389/fpls.2017.01713> PMID: 29046685
60. Martín M, Sabater B (2010) Plastid *ndh* genes in plant evolution. *Plant Physiology and Biochemistry* 48: 636–645. <https://doi.org/10.1016/j.plaphy.2010.04.009> PMID: 20493721
61. Ravi V, Khurana JP, Tyagi AK, Khurana P (2008) An update on chloroplast genomes. *Plant Systematics and Evolution* 271: 101–122.
62. Goulding SE, Olmstead RG, Morden CW, Wolfe KH (1996) Ebb and flow of the chloroplast inverted repeat. *Molecular and General Genetics* 252: 195–206. PMID: 8804393
63. Zhu A, Guo W, Gupta S, Fan W, Mower JP (2016) Evolutionary dynamics of the plastid inverted repeat: the effects of expansion, contraction, and loss on substitution rates. *New Phytologist* 209: 1747–1756. <https://doi.org/10.1111/nph.13743> PMID: 26574731
64. Vereecken NJ, Streinzer M, Ayasse M, Spaethe J, Paulus HF, Stoekl J, et al. (2011) Integrating past and present studies on *Ophrys* pollination—a comment on Bradshaw et al. *Botanical Journal of the Linnean Society* 165: 329–335.
65. Sedeek KEM, Scopece G, Staedler YM, Schönenberger J, Cozzolino S, Schiestl FP, Schlüter PM (2014) Genic rather than genome-wide differences between sexually deceptive *Ophrys* orchids with different pollinators. *Molecular Ecology* 23: 6192–6205. <https://doi.org/10.1111/mec.12992> PMID: 25370335
66. Hsu CC, Chung YL, Chen TC, Lee YL, Kuo YT, Tsai WC et al. (2011). An overview of the *Phalaenopsis* orchid genome through BAC end sequence analysis. *BMC Plant Biology* 11: 3. <https://doi.org/10.1186/1471-2229-11-3> PMID: 21208460
67. Leitch IJ, Kahandawala I, Suda J, Hanson L, Ingrouille MJ, Chase MW, Fay MF (2009) Genome size diversity in orchids: consequences and evolution. *Annals of Botany*, 104: 469–481. <https://doi.org/10.1093/aob/mcp003> PMID: 19168860